L-H Transition Threshold Physics at Low Collisionality

M.A. Malkov[1], P.H. Diamond[1], P.-C. Hsu[1], J. Rice[2], K. Miki[3] and G.R.Tynan[1]

[1]University of California, San Diego, USA
[2]PCFS, MIT, USA
[3]JAEA, Kashiwa, Japan

Corresponding Author: mmalkov@ucsd.edu

Abstract:
An L→H power threshold scaling including the minimum in $P_{th}\,(n)$ is discussed, elucidating an impact of inter-species energy transfer on threshold physics. Using a new four-field LH transition model, we study transitions in collisionless, electron heated regimes where the electron-ion coupling is allowed to be completely *anomalous*, due to the fluctuation of $\langle \mathbf{E}\cdot\mathbf{J}\rangle$ work on electrons and ions. New transition scenarios, characterized by the sensitivity of transition evolution to pre-existing L-mode profiles are also considered, using the new model.

1 Introduction

H-mode operation [1, 2] is the regime of choice for good confinement. This renders the questions of how to access, and remain in, H-mode critical. Foremost of these issues is the L→H transition power threshold and the related problem of hysteresis. To predict ITER transitions, one must understand the threshold in low collisionality, electron heated regimes where the physics may differ significantly from present day discharges. However, to properly understand the low-collisionality transitions it is important to extend the model beyond collisional coupling between the species. Therefore, in this paper, we discuss:

1. L→H *power threshold* scaling with special emphasis on the origin of the minimum in $P_{\rm th}\,(n)$ [3]. We elucidate the more general impact of inter-species energy transfer on threshold physics. Within collisional coupling between electrons and ions the minimum in the density scans of the power threshold has been studied recently in detail [4]. It is briefly discussed here to create a framework for studying the further two aspects of the L→H transition:

   (a) Transitions in collisionless, electron heated regimes where electron-ion coupling is *anomalous*, due to the fluctuations producing $\langle \mathbf{E}\cdot\mathbf{J}\rangle$ work on electrons and ions. A new element here is nonlinear flow damping which is dominant. A general theory of collisionless flow damping has been developed earlier [5].

2. New transition scenarios, characterized by the sensitivity of transition evolution to pre-existing L-mode profiles. This phenomenon is connected with the bi-stability range in the parameter space. The coexistence of L and H regimes for the same set of parameters makes a spontaneous or power-pulse-triggered $L \to H$ transition possible. To obtain such transitions using numerical model, an analytic identification of the phase coexistence domain is crucial.

To study the phenomena (2) and (3), we have developed a new numerical model. It differs, in a number of ways, from our previous 6-field model [4], that was primarily designed to study the collisionally dominated coupling between species and associated transitions, as well as its 5-field predecessor described earlier in detail in [6]. The new model is lightened in terms of the number of fields it evolves, thus focusing on the most important such fields. We removed the density and the mean flow velocity evolution from the model as deeming less important for the goal. Thus, transitions will occur in a fixed density profile, so the model will be useful in studying I-mode. We may then focus on the anomalous coupling between electrons and ions and isolate the inter-species thermal coupling phenomena in low density and low-collisionality regimes, relevant to ITER operation. Another justification of this system reduction is that the present four-field model can be studied analytically relatively easily, compared to the previous six-field model that makes identification of the transition trigger much more difficult, given the complicated form of collisionless coupling. Finally, the new model is improved on computing, which is now much better suited for a required description of rapidly propagating sharp fronts, as it utilizes adaptive space-time meshes.

1.1 Power Threshold Scaling.

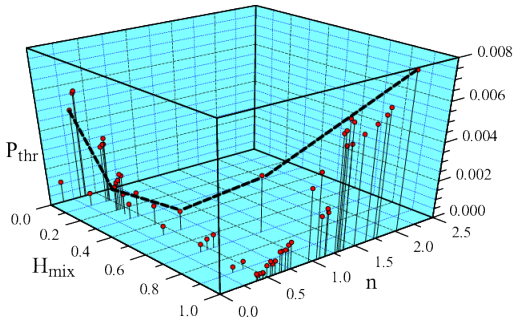

FIG. 1: 3D scatter plot of transition power threshold $P_{\rm thr}$ in heating mix-density variables. Note that the projection of the curve on the $(P_{\rm th}, n)$-plane has a clear minimum.

Our previous reduced model independently evolved the collisionally coupled electron and ion temperatures, along with density, turbulence intensity and flow profiles [4]. Extensive studies of the model have revealed the physics of the power threshold minimum in density. Fig.1 shows the power threshold plotted in 3D vs density and electron-ion heating mix. The dotted curve shows that *a minimum in $P_{\rm th}(n)$ originates from a combined effect of the density dependence of collisional electron-ion coupling and the electron-ion heating mix.* Specifically, the $P_{\rm th}$ decrease with growing n occurs due to collisional electron-ion heat transfer *and* an increase in ion heating. These serve to pump the edge ∇P_i, and thus the edge electric field shear. The ion heat flux at the edge is critical for the

transition. The high-density *increase* in threshold power appears as a consequence of increased flow damping. In all cases, the ion channel (directly or via electron coupling) is ultimately responsible for transitions. The role of the ratio $\tau = \tau_{Ee}/\tau_{\rm equ}$ (i.e. electron energy confinement time to collisional equilibration time) emerges as crucial parameter which governs the transition. For $\tau < 1$, there is no electron heated transition. More generally, this consideration shows that the threshold is not determined by edge physics alone, as frequently thought. Rather, the transition involves the global transport dynamics and species coupling as well.

This reinforces the role of energy transfer in the threshold.

1.2 Collisionless Regime Transitions

Ongoing studies are concerned with understanding the transition in the *collisionless regime*. This challenging regime presents at least two problems:

1. The electron-ion coupling is now *anomalous,* due to $\langle \mathbf{E} \cdot \mathbf{J} \rangle$ work

2. the shear flow damping is turbulent, and not due to collisional drag.

To address (1) we have extended a model of collisionless (i.e. anomalous) power coupling between electrons and ions. Most notable in this model are the absence of a coupling simply proportional to $T_e - T_i$, and the intensity dependence of the power coupling. To address (2) we have extended a recently developed theory of minimum enstrophy relaxation [7] which predicts that the flow damping should have the form of a turbulent *hyper-viscosity*. This nonlinear flow damping leads to additional turbulent viscous heating of the ions.

Preliminary results of studies of collisionless regimes suggest that L→H transition occurs when an *anomalous electron-ion thermal coupling front* attached to a propagating turbulence intensity *arrives at the edge*. The transition occurs when the front hits the edge and impulsively raises T_i there, thus raising ∇P_i, and the diamagnetic electric field shear, and so triggering the transition. Further studies of this interesting and relevant phenomenon are ongoing. This study highlights the importance of collisionless energy transfer process to transitions in regimes of ITER relevance.

1.3 New Transition Scenarios

Using the 4-field model, we are exploring new transition scenarios. New studies have revealed that a spontaneous transition can occur *in the absence of turbulence driven shear flow*. The key point here is the sensitivity of the transition to the pre-existing L-mode *density profile*. Ongoing work is focused on understanding this sensitivity and how to exploit it to optimize the access to H-mode. Our aim is to map the basins of attraction for different transitions. Now we turn to a brief description of the key physical elements included into the new 4-field model.

2 Four-field model for LH transition

2.1 Units, parameters, rescaling, and notation

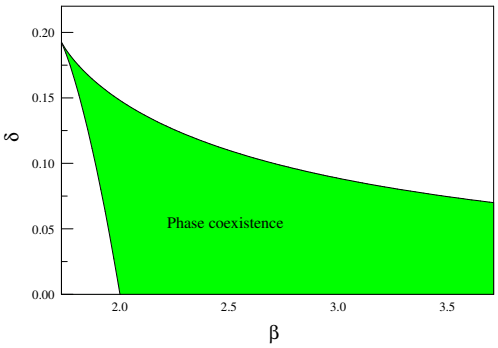

FIG. 2: Phase coexistence domain

To make the model manageable, we introduce some dimensionless variables and parameters along with certain simplifications. So, the units for time, length and other quantities are as follows: $[t] = a^2/C_s^2\tau_c$, $[x] = a$, where $C_s = \sqrt{T_{e0}/M} = const$ and a is the minor radius. Where it is needed, C_s will retain its temperature dependence. T_{e0} is the edge constant temperature and τ_c is also constant here. Furthermore, $[\chi^{e,i}_{neo}] = C_s^2\tau_c$, $\frac{M}{2m}\tau_e C_s^2\tau_c/a^2 \equiv \tau$, $\left[L_{T_{i,e}}, L_n\right] \equiv 1/\kappa_n$. The remainder of notation is as follows: $\gamma_c = n\gamma_{c0}/T_i^{3/2}$, $\tau = \tau_0 T_e^{3/2}/n$, $n = n_0\left(1-\beta x^2\right)$, $\kappa_n = -2\beta x/\left(1-\beta x^2\right) = d\ln n/dx$. We normalize n and other density dependent variables, such as γ_c, to n_0, but the dependence of collision time on density and temperature is retained and, as shown above, the respective quantities contain a factor $T^{3/2}/n$. In out simulations of the system dynamics, we will adjust all the parameters to obtain physically reasonable behavior. Then we will verify that the parameter values can emerge from reasonable combinations of the values n, T, etc.

3 Equations

As pointed out earlier, the new model evolves the electron and ion temperatures $T_{e,i}$, drift wave (DW) turbulence intensity, I , and zonal flow (ZF) velocity W :

$$\frac{\partial T_e}{\partial t} = \frac{\partial}{\partial x}\left(\frac{I}{1+\alpha_t R} + \chi^e_{neo}\right)T_e' - \frac{1}{\tau}\left(T_e - T_i\right) + S_e' + \gamma_{e0} I\left(\kappa_n + \sigma T_e'/T_e\right) \tag{1}$$

$$\frac{\partial T_i}{\partial t} = \frac{\partial}{\partial x}\left(\frac{I}{1+\alpha_t R} + \chi^i_{neo}\right)T_i' + \frac{1}{\tau}\left(T_e - T_i\right) + S_i' - \gamma_{e0} I\left(\kappa_n + \sigma T_e'/T_e\right) + \gamma_v I W'^2 \tag{2}$$

$$\frac{\partial I}{\partial t} = \left(\gamma_L - \Delta\omega I - \alpha_0 W^2/2 - \alpha_v R\right) I + \chi_N\left(I'^2 + I\cdot I''\right) \tag{3}$$

$$\frac{\partial W}{\partial t} = \frac{\alpha_0 I W}{1+\zeta_0 R} - \gamma_c W + \gamma_v\left(I'W' + IW''\right) \tag{4}$$

In this initial study of the new model, we adopt a simplified version of the transport suppression factor R, which is strictly valid for a strong thermal coupling between the species ($T_e \approx T_i$), be it anomalous and collisional. As the work on this model progresses we will relax the above limitation. So, currently the transport and DW instability suppression factor in eqs.(1-4) is used in the following simplified form

$$R = \left[\kappa_n \left(\kappa_n T + T'\right)\right]^2, \quad \text{with } \; T \equiv T_i + T_e.$$

The heat sources of electrons and ions are

$$S'_{e,i} = \frac{2S'_{0e,i}}{\sqrt{\pi} D_{e,i} \left[\text{erf}\left(\left(1 - a_{e,i}\right)/D_{e,i}\right) + \text{erf}\left(a_{e,i}/D_{e,i}\right)\right]} \exp\left[-\left(\frac{x - a_{e,i}}{D_{e,i}}\right)^2\right]$$

while the ITG and CTEM instabilities contribute to the linear growth rate of DW as follows: $\gamma_L = \sqrt{T_e}\left[\gamma_{L0} \Re\sqrt{-T'_i/T_i - T'_{i0}} - \gamma_{e0}\left(\kappa_n + \sigma T'_e/T_e\right)\right]$. The conventionally used ZF amplitude is $E_0 = W^2/2$. The shear flow velocity that enters the suppression factor is $V_E = \left(c/eBn\right) p'$, $p = n\left(T_e + T_i\right)$, $\left\langle V_E \right\rangle' \approx -\left(c/eB\right)\kappa_n\left(\kappa_n T + \kappa_n\right)$. Other notations are standard and have already been described in refs.[6, 4].

4 Stationary analytic solutions

First we seek for a steady-state solution, in the limit of small $\tau \to 0$. The strategy behind our solution is to assume that the turbulent components sit at their thresholds: $\gamma_v = \chi_N = 0$. The boundary conditions are set to zero gradients (stress free); otherwise the code will develop a wall-type dissipative instability and cannot be verified. A steady state solution is then described by equations for $T_{e,i}\left(x\right)$, I and W, obtained from eqs.(1-4) by setting $\partial_t = 0$. For $\tau \ll 1$, one should expect $T_e = T_i + \mathcal{O}\left(\tau\right) \approx T/2$. By adding these equations and using eq.(4), we obtain

$$\left(\frac{\zeta_0 - \alpha_t}{1 + \alpha_t R} R + \chi\right) T' + \frac{\alpha_0}{2\gamma_c}\left(\chi_i - \chi_e\right)\Delta T' - S = const$$

where we denoted $\Delta T = T_i - T_e$, $\partial S/\partial x = -\alpha_0\left(S'_e + S'_i\right)/\gamma_c$ and $\chi = 1 + \left(\chi^i_{neo} + \chi^e_{neo}\right)\alpha_0/2\gamma_c$. Assuming here $\left|\Delta T\right| \ll T$, we have

$$\left[\chi - \frac{\alpha\left(\kappa_n T + T'\right)^2}{1 + \omega\left(\kappa_n T + T'\right)^2}\right] T' = S\left(x\right) \tag{5}$$

where $\alpha = \left(\alpha_t - \zeta_0\right)\kappa_n^2$ and $\omega = \alpha_t \kappa_n^2$. The integration constant in S is chosen such that $S\left(0\right) = 0$, by virtue of the thermoinsulation at the boundary $x = 0$ (symmetry axis), $T' = 0$.

4.1 Flux-driven transitions

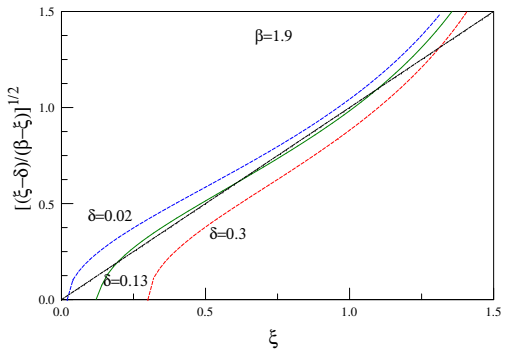

FIG. 3: Graphic illustration of the bifurcation diagram, shown in Fig.2. The three curves correspond to the r.h.s. of eq.(10) drawn for three values of δ that represent, respectively, an L-mode solution, LH coexistence phase, and the H-mode solution. These values of δ are taken from the region below the shaded (phase-coexistence zone), from that zone, and from the one above it.

Consider a situation in which the heat sources $S'_{e,i}(x)$ are localized near the origin ($x = 0$, i.e., core plasma). Then, the function $S(x)$ levels off at $x > L_h$, where L_h denotes the heat deposition radius and S can be considered constant beyond this point. For simplicity, and with no loss of generality, we may assume that $S = const$, for all $x > 0$. So, here we consider flux-driven transitions. That is, when the function S in eq.(5) is constant, the solutions $T = T(x)$ of this equation will depend on five independent parameters: χ, α, ω, κ_n and S. Of course, we are most interested in bifurcations of these solutions. A general bifurcation problem in five free parameters is clearly unmanageable, so we ultimately reduce this number down to two. To preserve contact with the physical formulation, however, we make this reduction step by step, rescaling first x to L_n; so, we introduce the following transformations $\kappa_n x \to x$, $S/\kappa_n \to S$, $\kappa_n^2\alpha \to \alpha$,$\kappa_n^2\omega \to \omega$. The range of x is now $\kappa_n < x < 0$, assuming $\kappa_n < 0$. Note that, this transformation merely transfers one free parameter to the boundary condition which is still useful in studying local bifurcations. Eq.(5) then rewrites

$$\left[\chi - \frac{\alpha\left(T+T'\right)^2}{1+\omega\left(T+T'\right)^2}\right] T' = S = const \tag{6}$$

The boundary condition for the last equation at the edge is $T(\kappa_n) = T_1$ which is set by the definition of the boundary value problem given in eqs.(1-4). Note that the boundary value $T(0) = T_0$ may be determined only after the complete solution $T(x)$ is obtained.

Now that both T and T' are positive, as S also is, we solve the last equation for $T(T')$ as follows:

$$T = c\sqrt{\frac{T'-a}{b-T'}} - T' \tag{7}$$

where

$$a = S/\chi, \quad b = S/\left(\chi - \alpha/\omega\right), \quad c = \left(\omega - \alpha/\chi\right)^{-1/2}$$

It follows that $a < T' < b$. Eq.(7) represents the original transport bifurcation in a three

dimensional parameter space (a, b, c). From this equation we obtain the following profile of the total temperature gradient $T' = T_e' + T_i'$.

$$x\left(T'\right) = x_0 - \ln\left|T'\right| + \tag{8}$$

$$\frac{c}{b}\left\{\sqrt{\frac{T'-a}{b-T'}} + \frac{b-a}{2\sqrt{ab}}\left[\tan^{-1}\frac{T'-\sqrt{ab}}{\sqrt{\left(b-T'\right)\left(T'-a\right)}}\right] - \left[\tan^{-1}\frac{T'+\sqrt{ab}}{\sqrt{\left(b-T'\right)\left(T'-a\right)}}\right]\right\}$$

Now, eqs.(7) and (8) determine the temperature profile $T\left(x\right)$ in a parametric form in which the parameter is T'.

However simple the above method of solving eq.(7) for $T\left(x\right)$, we still need to resolve this equation for $T'\left(T\right)$ for properly imposing the boundary conditions. Physically, the temperature is given at the edge, so we need T' at $x = -\kappa_n$ (the edge position in new variables introduced above) to determine the integration constant in eq.(8) and fully resolve the bifurcation problem considered. To solve eq.(7) for T' in a manageable way, further transformations are required, as the number of quantities it contains (five) is quite large. We first reduce this number to three by using the following variables

$$\xi = \left(T' + T\right)/c, \quad \delta = \left(a + T\right)/c, \quad \beta = \left(b + T\right)/c \tag{9}$$

Eq.(7) then rewrites

$$\xi = \sqrt{\frac{\xi - \delta}{\beta - \xi}} \tag{10}$$

Using the above relations, the phase coexistence condition can be written as follows

$$\frac{2}{27}\max\left[0, \beta\left(\frac{9}{2} - \beta^2\right) - \left(\beta^2 - 3\right)^{3/2}\right] \leq \delta \leq \frac{2}{27}\left[\beta\left(\frac{9}{2} - \beta^2\right) + \left(\beta^2 - 3\right)^{3/2}\right], \quad \beta \geq \sqrt{3} \tag{11}$$

The respective domain on the (β, δ) plane is shown in Fig.2. If the parameters (β, δ) lie outside of the phase-coexistence domain, only one solution out of the three possible in eq.(10) is real. In particular, for $\beta > \sqrt{3}$ it corresponds to an H-mode solution, as shown in Fig.3 with the lower dashed curve. For $\beta \leq \sqrt{3}$, we obtain an L-mode solution, as it corresponds to the lowest real T' value out of the three solution with the other two roots becoming complex.

Using the above bifurcation analysis, we will study spontaneous and pulse/noise driven LH transitions. By choosing the system parameters within the phase-coexistence domain, we have already obtained such transitions, with a preliminary example shown in Fig.4. The initial state clearly belongs to a stable L-mode, as no kink in the temperature profile is present and the stationary solution persists for some time. However, a spontaneous transition to a stable H-mode occurs in the range $3 < t < 5$ when the system develops such kink in the temperature profile. A short heat pulse is applied around 2/3 of the

full integration time, but leaves the H-mode essentially unchanged. The next step in this ongoing work will be relaxing an artificially enhanced temperature equilibration between electrons and ions, before studying the spontaneous transitions in more detail.

5 Conclusions

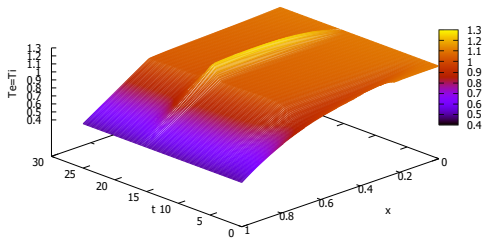

FIG. 4: Spontaneous LH transition with suppressed shear flow.

A new analytical and numerical 4-field model for describing $L \to H$ transitions in weakly collisional ITER-related regimes is developed. It evolves electron and ion temperatures, drift wave and zonal flow energies. A new type of transition scenario, which is more sensitive to the pre-existing L-mode structure than to the power variation near the threshold is identified. Dynamical realization of such transitions became possible after an accurate analytic determination of the phase coexistence domain and transition criteria in a multi-dimensional parameter space of the system. Stationary solutions of the model, obtained analytically for that purpose, are also crucial for the code verification. The work studying dynamical evolution of $L \to H$ transitions numerically is ongoing.

Acknowledgments The work supported by the US Department of Energy under Award No. DE-FG02-04ER54738.

References

[1] Wagner, F., et al *Physical Review Letters* **49**, 1408–1412 November (1982).

[2] Burrell, K. H., et al *Physics of Plasmas* **12**(5), 056121 (2005).

[3] Ryter, F., Orte, L. B., Kurzan, B., McDermott, R., Tardini, G., Viezzer, E., Bernert, M., Fischer, R., and Team, T. A. U. *Nuclear Fusion* **54**(8), 083003 (2014).

[4] Malkov, M. A., Diamond, P. H., Miki, K., Rice, J. E., and Tynan, G. R. *Physics of Plasmas* **22**(3), 032506 #mar# (2015).

[5] Zhao, L. and Diamond, P. H. *Physics of Plasmas* **19**(8), 082309 August (2012).

[6] Miki, K., Diamond, P. H., Gurcan, O. D., Tynan, G. R., Estrada, T., Schmitz, L., and Xu, G. S. *Phys. Plasmas* **19**(9), 092306 (2012).

[7] Hsu, P.-C. and Diamond, P. H. *Physics of Plasmas* **22**(3), 032314 March (2015).